Separation and Purification Technology 269 (2021) 118777

Contents lists available at ScienceDirect

Separation and Purification Technology

journal homepage: www.elsevier.com/locate/seppur

Detailed modeling of solids separation by microsieving in a rotating belt filter: Explicit effect of particle size, mesh size, and polymer dose

Furqan Ahmad Khan [a,c], Pankaj Chowdhury [b,c], Francesca Giaccherini [a,c], Anthony Gerald Straatman [a], Domenico Santoro [b,c,*]

[a] Department of Mechanical & Materials Engineering, Western University, London, Ontario N6A 5B9, Canada
[b] Department of Chemical and Biochemical Engineering, Western University, London, Ontario N6A 5B9, Canada
[c] Trojan Technologies, London, Ontario N5V 4T7, Canada

ARTICLE INFO

Keywords:
Cake filtration
Modeling
Microsieving
Primary wastewater treatment
Rotating belt filter

ABSTRACT

Microsieving by rotating belt filters is an engineered fractionation method for particle separation from wastewater that can be used as an alternative to primary clarification due to its smaller footprint and lower total cost of ownership. Because of the multiscale nature of the filtration processes involved, and the interdependent variables controlling performance and the system design, the availability of verified and comprehensively validated models that, based on fundamental principles, can explicitly capture the effect of particle size, mesh size and polymer dose are essential for performance optimization and scale-up. In this paper, a detailed microsieving filtration model was derived by extending Darcy's law to a dual-layer dynamic framework whose predictions were validated against batch (column) and continuous flow (RBF pilot) experimental data. The ability of the microsieving model to accurately capture observed trends confirmed that the model formulation, derived from column experiments, were sufficiently accurate and flexible to capture the relevant physics involved, with a relative error in performance scale up (from column to pilot) of 33% and 14% for filter capacity and effluent total suspended solids, respectively. Upon further calibration against pilot data, the relative error was reduced to 9% and 5%, respectively, indicating the suitability of the model structure in further adapting to filtration process conditions occurring at pilot scale. Finally, the calibrated model was used to derive guidance for future pilot studies. It was determined that, under naturally varying influent conditions, at least 8 h of continuous pilot data, with sampling frequency of at least 15 min for filter capacity and suspended solids concentration, were necessary for a satisfactory estimate of the model parameters.

1. Introduction

A large fraction (30–50%) of total suspended solids (TSS) in municipal wastewater is represented by cellulose fibers originating from toilet paper and cellulose-like material (hemicellulose and lignin) [1]. Previous studies have shown that cellulose can show very complex

Abbreviations: A, expandable mesh resistance coefficient, 1/m; B, expandable cake resistance coefficient, m^2/m^3; B_o, base cake resistance coefficient, m^2/m^3; b_t, cake resistance coefficient accounting for TSS_{in}; b_m, cake resistance coefficient accounting for mesh size; b_p, cake resistance coefficient accounting for polymer concentration; BCE, batch coefficient evaluation; CFV, cumulative filtered volume, m^3/m^2; $CFV_{model,I}$, model cumulative filtered volume for belt element-i, m^3/m^2; C_p, polymer concentration, mg/L; CWDC, clean water drainage column test; g, gravitational acceleration, m/s^2; h, height, m; Δh, difference in upstream and downstream water levels, m; K, permeability of the porous medium, m^2; K, expandable TSS equation coefficient, L/mg; k_1, base TSS equation coefficient, L/mg; k_2, TSS equation coefficient accounting for polymer concentration, L/mg; k_3, TSS equation coefficient accounting for mesh size; m_1, m1p, m_2, m2p, mesh resistance coefficients; ΔP, pressure drop per length, $(N/m^2)/m$; PC, pilot calibration test at Pottersburg WWTP, Canada; PCE, pilot coefficient evaluation; PV, pilot validation test at Pottersburg WWTP, Canada; R_{cake}, cake resistance, 1/m; R_{mesh}, mesh resistance, 1/m; R_{total}, total resistance, 1/m; Q_{exp}, experimental flow rate, L/s; Q_{model}, model flow rate, L/s; $Q_{model,I}$, model flow rate for belt element-i, L/s; T, time, s; TSS_{in}, upstream total suspended solids, mg/L; TSS_{out}, downstream total suspended solids, mg/L; U, flow velocity, m/s; WWTP, wastewater treatment plant; WWDC-1, wastewater column drainage test conducted at Sarnia WWTP, Canada; WWDC-2, wastewater column drainage test conducted at Pottersburg WWTP, Canada; Γ, TSS equation coefficient, m^2/m^3; Ω, belt speed, Hz; M, dynamic viscosity, $(N.s)/m^2$; P, density, kg/m^3; θ, belt inclination angle, degrees; η, microsieving mesh size, μm.

* Corresponding author at: Department of Chemical & Biochemical Engineering, Western University, London, Ontario N6A 5B9, Canada.
E-mail address: dsantoro@uwo.ca (D. Santoro).

https://doi.org/10.1016/j.seppur.2021.118777
Received 28 January 2021; Received in revised form 12 April 2021; Accepted 12 April 2021
Available online 18 April 2021

degradation kinetics, with degradation rates much slower than other organic particulate compounds, typically present in domestic wastewaters [2,3]. Moreover, the elongated morphological feature of cellulose fibers may limit the separation by gravity settling, as operated in a primary clarifier. To enhance the separation of these types of fibers, new technologies based on the capture of particulate by shape and size have been developed and have recently been introduced to the market (microsieves). The rotating belt filter (RBF), a microsieving technology, has been shown to have performance dependency on the particle size distribution in the influent wastewater as well as the mesh size and flow rate [4]. A clear benefit of RBF over primary clarifier is the much higher hydraulic loading that an RBF can sustain, leading to a much smaller footprint and lower capital cost, making RBF attractive in contexts where land is expensive or access to capital is limited.

RBFs operate on the mechanism of sieving and cake filtration, which allows for the removal of solid particles up to three times smaller than the pore size of the mesh [5]. Since the cake is formed due to particle accumulation on the mesh prompted by the size exclusion mechanism (i.e., the particle forming the cake are those greater in size than the mesh size), the cake filtration effect strongly depends on the particle size distribution of the influent wastewater. As a result, higher filtration efficiencies are obtained with RBFs for municipal wastewaters high in fiber content typically associated with the use and the discharge in the sewer of toilet paper. In the absence of toilet paper fiber in the influent wastewater, another strategy for increasing RBF particle removal efficiency is via pre-treatment by cationic polymers (i.e., polyacrylamide) which act as both a bridge and a coagulant among suspended particles. The use of polymer is crucial for sewage systems with a low content of fibers such as toilet paper. As such, RBF performance is highly dependent on influent wastewater quality, which makes it of paramount importance to use numerical models that can take into account the interplay between flow dynamics and particle separation as well as influent particle size distribution and mesh size.

First-principles models for cake filtration have been developed in previous studies [6–9]. However, these approaches were focused on modeling the process of cake filtration rather than scaling up the model to the entire filtration system unit. Later, other groups developed numerical models for filtration systems and correlated cake resistance, cake porosity, particle density, particle diameter, and cake solidity [5,10–17]. Most of the authors discussed and identified the limitations of a first-principles approach recognizing the complexity and disadvantages in estimating the mathematically dependent and statistically correlated parameters involved in the model. In addition, available models were developed primarily for constant flow or constant pressure, an assumption that is applicable for microsieving operated on inclined rotating belt filters. On the contrary, RBFs have spatially varying pressure head difference and cake resistance, leading to spatially dependent filtration performance as illustrated by DeGroot et al. with simplified hydrodynamic calculations verified against computational flow dynamics (CFD) simulations [18]. Sherratt et al. developed a numerical model to characterize the resistance across a mesh filter, using CFD modeling and the cake layer estimated by a gravity drainage experiment [19]. Through the combination of the two resistances, an integrated filtration model was developed to conduct parametric analysis on the performance of inclined RBF systems. Later, Boiocchi et al. [20] used the modeling framework developed by Sherratt et al. [19] to incorporate the dynamic effects of the pilot RBF system by modeling the transient phenomena associated with upstream and downstream water level variations using ordinary differential equations. Model parameters were evaluated by calibrating the model against the pilot RBF data, showing that the predictions were satisfactory both with and without pre-treatment by cationic polymers. However, this approach did not explicitly consider the effect of particle size of the influent solids or filtration mesh size, which are very important design parameters to consider when optimizing the RBF technology for accurate sizing.

In this paper, we extended the RBF filtration model reported in Sherratt et al. and Boiocchi et al. by incorporating the effects of sieving efficiency (a surrogate for particle size) and filter mesh size on the microsieving filtration process [19,20]. The extended model was based on the development of a new modeling framework centered on Darcy's law using a validated cake growth expression able to satisfactorily capture the mesh behavior both in particle-free water (i.e., tap water) and particle-rich wastewater. Moreover, by introducing power-law-based mathematical dependencies between water quality parameters and model coefficients, it was possible to successfully achieve scaling up of filtration performance from column gravity drainage and sieve tests to pilot-scale experiments. The validity of the model structure was also successfully tested against pilot data collected from various international locations (Canada, Korea, USA, and Australia) with very satisfactory results. Finally, the validated model was used to estimate, with an inverse modeling approach, the optimal length of a hypothetical pilot campaign so that the model parameters could be estimated with a reasonable level of uncertainty for a robust technology scale-up.

2. Materials and methods

2.1. Mechanism of rotating belt filtration

A schematic of a typical RBF system is shown in Fig. 1 [21]. The RBF system consists of influent and effluent wastewater streams separated by an angled rotating belt carrying a microsieving surface with pore sizes ranging from 50 to 500 μm (typical nominal pore size range: 150–350 μm), which performs the liquid and solids separation processes. The filtration process is driven solely by gravity, with the hydrostatic pressure (controlled by belt speed) acting on the influent side of the RBF unit. The accumulation of solids on the moving belt induces the formation of a thin cake, which creates resistance to filtration, allowing less wastewater to pass through the mesh. At the beginning of the microsieving process (i.e., in the absence of cake), the total resistance of the system corresponds to the clean mesh resistance only. However, with the dynamic formation of the thin cake made of suspended solids, the cake resistance starts to significantly contribute to the total resistance, making the contribution of the clean mesh vanishingly small. Therefore, as the filtration process spatially evolves from the bottom to the top of the rotating filter belt, the thickness of the cake continues to increase together with the total filter resistance while the specific capacity of the filter progressively decreases, as schematically shown in Fig. 1. This enables the cake filtration process to capture particles up to one third smaller than the nominal pore size of the microsieving mesh.

It is crucially important to comprehend the mode of operation of an RBF system to understand the filtration process occurring in a real WWTP. In general, good cake formation is anecdotally observed and reported when an RBF is operated at constant flowrate and uniform belt speed since those conditions would lead to minimal particle deposition disturbance. However, due to the constantly varying concentration of

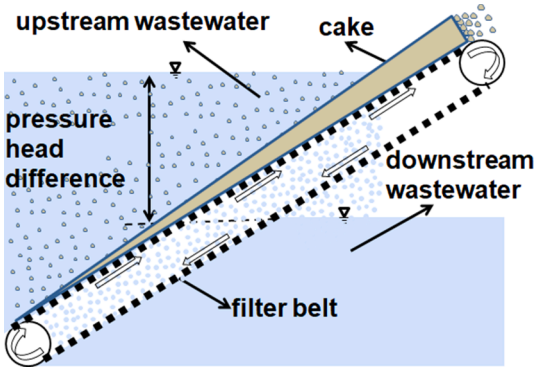

Fig. 1. Schematic of an RBF system and cake formation along filter belt carrying the microsieve.

total suspended solids in raw wastewater (TSS_{in}) and real plants, it is practically impossible to maintain constant operations without controlling the RBF variables dynamically. Instead, quasi-steady-state conditions are achieved by controlling the upstream water level using the rotational velocity of filter belt speed (ω) as a manipulated variable using a programmable logic controller. As an example, in the presence of a TSS_{in} increase, the upstream water level would also increase. Then, a water level sensor measures such an increase, and triggers a proportional increase of the belt speed to reduce the thickness of the cake (hence the total resistance to filtration) and reduce upstream water level at the desired setpoint. In essence, a faster rotation of the belt leads to a thinner cake layer resulting in lower TSS removal efficiency and higher filter capacity. Consequently, operating an RBF system at an optimal removal efficiency involves balancing solids removal and filter capacity under continuous variation in TSS_{in}, upstream water level, and belt speed. As a result, only quasi-steady-state conditions can be achieved, and a suitable modeling framework shall be constructed to accurately reflect those filtration dynamics into the conceptual model implemented to describe the RBF process.

2.2. Modeling framework and governing equations

The dynamic behavior of an RBF unit employing microsieves requires the filtration model to be capable of accounting for unsteady wastewater characteristics and input parameters. A quasi-unsteady modeling framework may also be acceptable to describe the microsieving particle separation process occurring in an RBF unit if one considers that the characteristic timescales of microfiltration (i.e., seconds to minutes) are considerably smaller than those associated with influent wastewater quality variabilities (i.e., hours to days). Therefore, a valid approach in modeling the microsieving entails the development of a modeling framework using a sequence of instantaneous steady states accounting for the dynamics of variation of wastewater quality, water level (i.e., the driving force to filtration), and belt speed (RBF-dependent variable affected by the system geometry and filtration angle). Under those assumptions, the governing equation for pressure and filtration velocity is given by the well-known Darcy's Law:

$$\Delta P = \frac{\mu U}{K} \tag{1}$$

where ΔP is the pressure drop across the length of the porous medium, μ is the dynamic viscosity of the fluid (water, in our case), U is the flow velocity through the porous medium, and K is the permeability of the porous medium. Furthermore, we consider filter mesh and cake as thin, porous media, which provide resistance to flow across the rotating belt. In this respect, Eq. (1) can be written in resistance form:

$$\Delta P = \mu U R_{total} \tag{2}$$

where, R_{total} is the total resistance to flow across the system (i.e., the sum of clean mesh resistance (R_{mesh}) against clean water and cake resistance (R_{cake})against wastewater).

The separation of R_{mesh} and R_{cake} is useful as the magnitude of the two resistances changes throughout the microsieving process and spatially too, given the rotating nature of the rotating belt filtration process. Initially, and near the bottom of the RBF unit (where the clean mesh is constantly re-introduced into the raw wastewater), R_{mesh} dominates R_{total} (due to lack of particles accumulated on the sieve). The opposite is true at the top of the RBF unit, where the thickest cake is present (i.e., near the end of the filtration cycle).

2.3. The total resistance concept: Model formulation and identification

While practical and useful in specific circumstances where water quality and particle size are relatively uniform and stable in time, the total resistance expression proposed in Sherratt et al. and subsequently adopted in Boiocchi et al. has some limitations [19,20]. The main one entails the non-physical behavior of the proposed expression for extreme conditions corresponding to thick cakes and high filtered volumes (for a single filtration cycle). This is because the total resistance expression R_{total} in Sherratt et al. is a function obtained from ratioing the primary variable modeled by the authors (i.e., the time-dependent water level in the column) and its derivative [19]. As a result, R_{total} is not guaranteed to be monotonic in the cumulative filtered volume and may behave strangely when extrapolated to a high value of filtered wastewater. To overcome this limitation, in this paper, we focused on the development of an RBF model that is centered around the a-priori selection of a family of mathematically suitable functions (having the desired and physically reasonable properties expected for cake filtration), with subsequent identification of the form of equation for the total resistance model R_{total} used in Eq. (2) against experimental data. Among the several functions tested (not all reported in this manuscript for brevity), the double exponential function has shown very promising results (Fig. 2).

In the case of double exponential models, R_{total} can be described as:

$$R_{total} = A.e^{e^{CFV.B}} \tag{3}$$

where, CFV is the cumulative filtered volume, and A and B are model coefficients. CFV is normalized by the filtration surface area, which means that it has units of m^3/m^2. It should be noted that in Eq. (3), the R_{total} equation accounts for both cake and clean mesh resistances; however, these two resistances can be appropriately isolated, as explained in the next section of this manuscript. Mathematically, Eq. (3) returns the clean mesh resistance when B is set to zero, which allows Ae to characterize the mesh resistance. It is essential to emphasize that the double exponential expression used in Eq. (3) to expand R_{total} has also been compared against experiments, as shown in Fig. 2. In there, R_{total} has been quantified using a column test apparatus where drainage experiments were carried out on a representative sample of raw wastewater and a circular sample of a real microsieve. As anticipated, the dead-end nature of the filtration experiments returns the expected behavior typical of very rapid growth in the total mesh resistance R_{total} which could not have been captured by a single exponential expression. Specifically, a double exponential function was found to capture the R_{total} very well with the experimental data, as shown in Fig. 2.

Substituting Eq. (3) in Eq. (2), and replacing $\triangle$P with $\rho g \triangle$h, we obtain Eq. (4):

$$\rho g \Delta h = \mu U (A e^{e^{CFV.B}}) \tag{4}$$

Eq. (4) is the governing equation for the microsieving process of raw wastewater carried out in an RBF unit. It states that flow through a microsieve is directly proportional to the differential hydrostatic

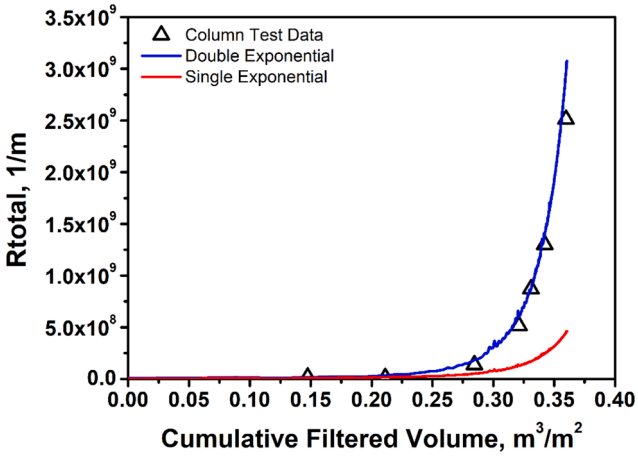

Fig. 2. Total resistance R_{total} versus CFV for the single and double exponential function.

pressure and inversely proportional to the total resistance offered by the combined media formed by the clean microsieve mesh and thin cake. For the case of an RBF unit operated with constant upstream water level controlled by the belt speed, the Δh (at the left-hand side of Eq. (4)) can be quantified, as a first approximation, from the RBF system geometry. On the right-hand side, we have flow velocity (U) and the steady-state and local value of the total resistance (which are unknown and must be estimated). Since U can be written as a function of H, the problem can be mathematically solved once A and B are known.

2.4. Model extension to particle size, mesh size, and polymer dose

RBF performance is reported to be highly dependent on the average particle size in the raw wastewater and the average pore size of the microsieve used in the system. Therefore, a useful RBF model must be capable of predicting the impact of these two important process variables. To accomplish this, the first step is to extend the model to capture the effect of particle size and pore size, which represents the main contribution to the state of the art offered by this paper. In our current study, this was achieved by parameterizing the model coefficients expected to be dependent on mesh size and pore size with extended power laws, as also suggested by Boiocchi et al. [20]. In Eq. (4), the B coefficient is certainly particle size and mesh size-dependent, as it captures how the filter cake that grew on the microsieves changes along the filter belt (a phenomenon that is affected, among others, by the interplay between particle and microsieve sizes). Therefore, the B coefficient of Eq. (4) was expanded, as shown below:

$$B = \frac{B_o TSS_{in}^{\ b_t}}{\eta^{b_m}} \tag{5}$$

where, B_o is the reference cake resistance coefficient (i.e., the value assumed by the B coefficient when TSS_{in} and mesh size are both unity), b_t is the power-law coefficient of the variable TSS_{in}, and b_m is the cake resistance coefficient of the mesh size (η) variable. Through this expansion, the model can now capture the variation in TSS concentration and mesh size associated with the microsieving filtration process. From a filtration process perspective, the selection of an expression like what reported in Eq. (5) seems logical since high TSS value will induce the thicker and denser cake (hence a higher cake resistance represented by a higher B coefficient), while conversely, microsieves with bigger mesh size would generate a more porous cake and lower cake resistance to flow (hence a lower B coefficient). A similar thought process could be applied to the expansion of the B coefficient to capture pre-treatment by coagulants and polymers. Indeed, the formation of bigger particles before the microfiltration process is expected to lead to a higher reference value for B_o, which can now be expanded into $B_o + b_p C_p$. It should be noted that the assumption made in assuming a linear relationship between Bo and polymer dose holds true if the cake porosity and the overall cake structure remains the same. Moving from a suspension type to another may require a re-verification of this assumption and a re-calibration of the empirical coefficients reported in the power law equations used in this paper.

When directly substituted to B_o in Eq. (5), the expanded expression reported in Eq. (6) is obtained:

$$B = \frac{\left(B_o + b_p C_p\right) TSS_{in}^{\ b_t}}{\eta^{b_m}} \tag{6}$$

where C_p represents the polymer concentration used in the process and b_p accounts for increment in cake resistance due to polymer. It should be further pointed out that b_m and b_t are empirical correction coefficients; therefore they are expected to be influenced by particle characteristics and fluid properties. That said, these coefficients can be expected to be relatively constants for municipal wastewater applications as long as the particle characteristics does not dramatically change from one site to another.

Finally, the last step associated with the extension of Darcy's law to pore size and mesh size entails the extension of the particle removal efficiency of a static process (sieve test experiment, a surrogate test for finding the average particle size of the influent wastewater) towards a dynamic filtration process as the one occurring in an RBF unit. To do so, we imagine decomposing the filter belt in a sufficiently high number of elements and modeling each of these individual subsystems as independent column drainage experiments (as shown in Fig. 3). If the sieve experiment is repeated for different initial values of the influent TSS concentration and mesh sizes, it is possible to obtain a parametric sieve test filtration kinetic model connecting pore size and mesh size to CFV, that is, the bridging variable between static and dynamic filtration processes. In Eq. (7), the mathematical expression required to model sieve test experiments is reported:

$$TSS_{out} = TSS_{in} e^{(-k.TSS_{in})} e^{(-\gamma.CFV)} \tag{7}$$

where TSS_{out} is the filtrate TSS concentration of the sieve test, and k and γ are water-quality specific cake-specific parameters.

From the above expression, the sieving efficiency can be defined (and mathematically determined) as $TSS_{in} e^{(-k.TSS_{in})}$ by setting CFV to be zero, which represents the fraction of particles removed by the sieve (mesh) by capturing particles greater than the mesh size. In the case of chemical pre-treatment with polymer, it is expected that an increase in the average particle size will correspond to an increase of the sieving efficiency captured by parameter k of Eq. (7). With considerations like those reported for Eq. (6), the effect of mesh size η and polymer concentration C_p can be incorporated in Eq. (7) by expanding the k coefficient as follows:

$$k = \frac{k_1 + k_2 C_p}{\eta^{k_3}} \tag{8}$$

2.5. Model simulation procedure

To simulate the filtration process, we first need to evaluate the model coefficients related to clean mesh (as those will not be changed during wastewater filtration simulations), and then the model coefficients describing the variation of cake resistances as a function of time (or, in our case, cumulative filtered volume). Moreover, to predict removal efficiency, we need to find, via a series of sieve test, the coefficients required in the TSS_{out} expression reported in Eq. (7) and convolve it with the steady-state solution of flow (or, in our case, cumulative filtered volume) obtained from the extended version of Darcy's law.

There are two procedures that are potentially viable to estimate the cake resistance and the sieving removal coefficients required for the microsieving filtration process simulation, each with its advantages and disadvantages. In the first approach, termed as batch coefficient evaluation (BCE) method, the coefficients are estimated using data generated with batch column drainage experiments using real wastewater from the specific wastewater plant of interest. This is mostly a sizing procedure that is utilized when pilot data are not available. This approach can be executed quickly (less than one hour, including column set-up and data processing) but shows an error ranging from 10 to 30% in the filter capacity and solids removal efficiency. An alternate method consists of short-term pilot data to collect the (dynamic) data required for solving the inverse problem (from integrated quantities to model coefficients). This approach is termed as pilot coefficient evaluation (PCE) method. In this respect, all the required parameters such as TSS_{in}, TSS_{out}, belt speed, flow rate, and water level are logged approximatively every 15 min, and then used to estimate the model coefficients using a global optimization search algorithm in the space of the model coefficients.

Once the model coefficients are determined, Eq. (4) can be solved along the filter belt to simulate the entire RBF process cycle and estimate the quantity of interest. In this respect, the filter belt is discretized into a

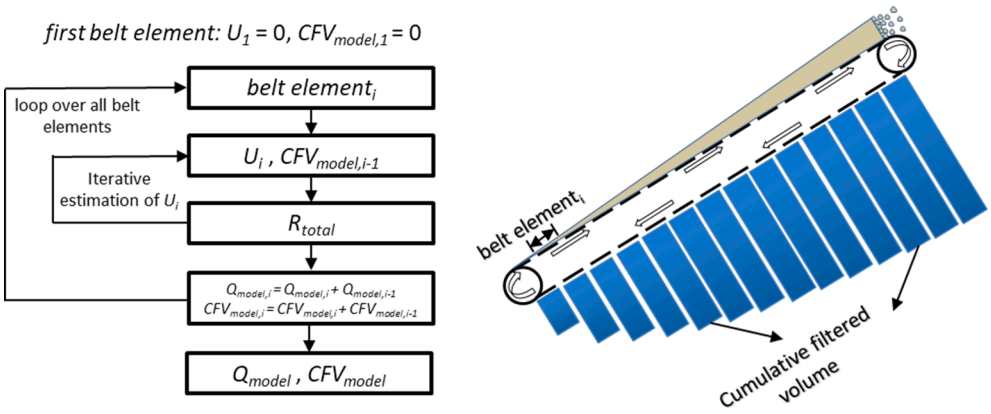

Fig. 3. Solution procedure of the developed filtration model.

sufficiently large number of elements (in this paper we used 500 elements, as doubling the filtration elements to 1,000 only improved solution accuracy by 1%), which also enables the model to account for the blockages imposed by the supporting structure under the belt. Subsequently, Eq. (4) is solved for each element, as shown in Fig. 3. For the first element, we consider $CFV_{model,1} = 0$ and $U_1 = 0$ to evaluate R_{total} using Eq. (3), followed by the estimation of U_1 using Eq. (4). Since the proper value of U_1 is required to obtain R_{total}, its converged value is obtained iteratively. Once U_1 is calculated, it is multiplied by the single element area to get the $Q_{model,1}$. The evaluation of $CFV_{model,1}$ is also dependent on filtration velocity U, element area, belt speed (ω), and belt angle (θ). For the adjacent element, we consider CFV_{model} of the previous element and again apply Eq. (3) to obtain the resistance of that element. Thus, $Q_{model,i}$ and $CFV_{model,i}$ are estimated for each belt element and cumulatively added up to the last belt element to obtain the total Q_{model} and CFV_{model}. Once CFV_{model} is evaluated, the predicted TSS_{out} is obtained using Eq. (7).

In the present work, we applied this modeling framework and simulation process to pilot the filtration data obtained using a SF2000 RBF model (details mentioned in Table SI1), a commercial system manufactured by Salsnes Filter (Norway) [21]. As such, the design parameters used in the simulation, including upstream and downstream water levels, belt length, belt width, belt inclination angle, and mesh size, were all based on the SF2000 model series.

2.6. Experimental datasets and procedures

Several sets of experiments were conducted and used in this study for model development and validation, namely, gravity drainage column tests, sieve tests, and pilot tests.

The gravity drainage column tests allow for characterizing the gravity-based filtration process. The first step is to conduct them with clean water (CWDC, $TSS_{in} = 0$ mg/L) to allow the estimation of the clean mesh resistance parameters (m_1, m1p, m_2, and m2p) included in Eq. (13). Subsequently, identical column drainage tests are performed with real wastewater (WWDC-1 and WWDC-2) to evaluate the cake resistance parameters (B_o, b_t, and b_m), included in Eq. (5).

Wastewater sieve test (WWS) allows for the estimation of the particle size distribution and consists of filtering known volumes of raw wastewater (sufficiently low to avoid cake formation) through a series of filter meshes of known pore sizes. The same test could be operated by filtering known aliquots cumulatively, thus allowing for the estimate of cake-growth water-quality-specific model parameters (k and γ) as shown in Eqs. (7) and (8), as mentioned in Section 2.4.

Finally, pilot calibration tests (PC) were performed for the SF2000 system using 350 μm mesh, with and without polymer, to calibrate further the model parameters estimated from the column tests. Furthermore, pilot validation tests (PV) were also performed with the SF2000 system using 350 μm mesh, utilizing two approaches to validate the sizing methodology. The latter was checked against three international locations from which Salsnes filter pilot data were available. Experimental procedures are briefly discussed in the following sections and reported in more detail in the supporting information file (Table SI2).

2.6.1. Column and sieve tests

Drainage column tests were performed with a vertical cylindrical column as described in Sherratt et al. [19], where a well-mixed sample of wastewater is filtered through a column with the mesh being installed at the bottom (Fig. 4a). Different mesh sizes (between 54 and 840 μm) were used in the drainage column tests. In the case of a clean water column test, standard tap water was used. An ultrasonic sensor was employed to monitor the height of wastewater with the help of Senix view software (Hinesburg, USA). During the filtration process, the change in the wastewater column height (as a function of time) was recorded to evaluate mesh and cake resistances. In the case of CWDC, the rate of change of column height was derived, and the mesh resistance coefficients were assessed with 70 drainage tests. For WWDC, the cake resistance was evaluated for wastewater from two different WWTPs.

Analogous to the drainage column test, sieve tests were performed to evaluate the TSS_{out} equation coefficients. The experiment involved taking a sample of wastewater with known TSS_{in} and then sieving it through the filter mesh to obtain TSS_{out} and CFV.

2.6.2. Pilot tests

The cake resistance and TSS_{out} model coefficients were evaluated using the logged pilot data using PCE method. For the PC dataset, the pilot unit comprised of SF2000 with PLC controller, flow meters, and the connected piping and sampling valves (Fig. 4b). The RBF unit was tested with different filter mesh (belt) sizes and was run in automatic mode during the test. Under automatic mode, the belt speed automatically adjusted to maintain a pre-set water level in the RBF, given the varying influent flow rates. The TSS_{in} and TSS_{out} were measured by collecting samples after the system achieved a steady state. During the pilot run, the data logger recorded the RBF parameters (belt speed, water level, etc.) and $TSS_{in/out}$ values.

The filtration model was validated using both the BCE and PCE methods. In the BCE method, which uses only batch experimental data, a set of drainage column and sieve tests (WWDC-2 and WWS) carried out at Pottersburg WWTP was used to estimate the model coefficients. Once the model coefficients were determined, the model was simulated against pilot data (PV), which was also generated at the Pottersburg facility. The PCE method involves obtaining the model coefficients from the pilot data (PC) using an inverse calibration method, followed by simulating the model for the PV dataset.

To further test the applicability of the model to a wide range of

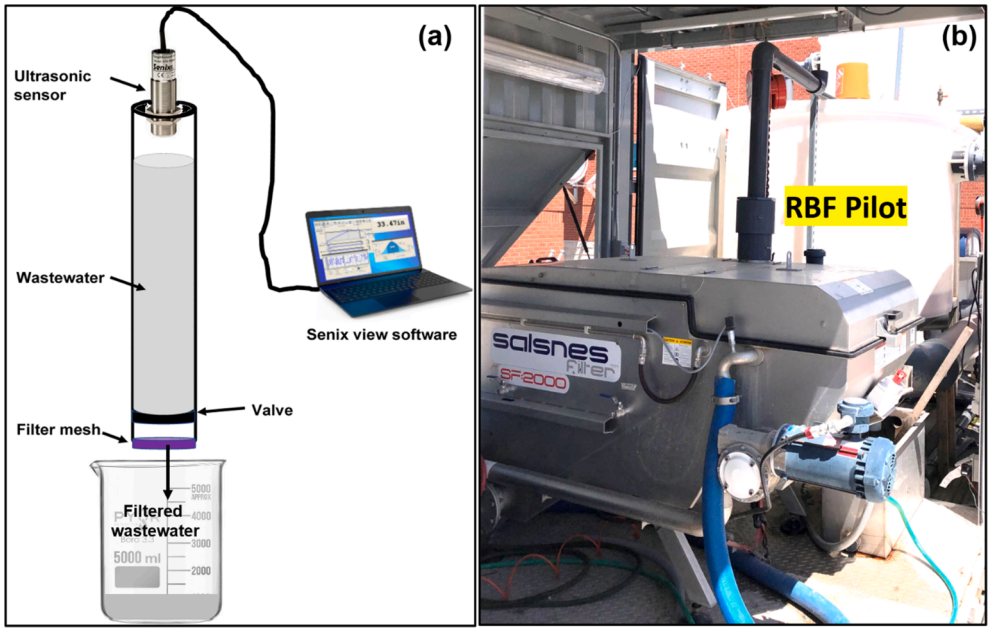

Fig. 4. In the picture: (a) Drainage column test and (b) RBF pilot set up.

influent wastewater characteristics, we applied our model to pilot data which were obtained at different locations. Those calibration data were collected from international pilot locations (Korea, USA, and Australia).

3. Results and discussion

3.1. Evaluation of clean mesh resistance

Before we estimate the cake filtration model coefficients, it is essential to evaluate and fix the mesh resistance against clean water (clean mesh resistance). Clean mesh resistance was evaluated by performing the gravity drainage column tests with clean water. As expected, the smaller the mesh size, the longer the time to drain, due to higher resistance of small pores to flow compared to the larger mesh size. To estimate clean mesh resistance, the Eq. (3) can still be used since it reduces to

$$R_{tot} = R_{mesh} = Ae \tag{9}$$

With no formation of cake, R_{tot} reduces to Ae, which represents total resistance offered by the mesh that includes the effects of mesh porosity, belt thickness and surface smoothness. Moreover, as observed by Sherratt et al. [22], R_{mesh} is dependent on flow velocity, and can be written as

$$R_{mesh} = m_1 + m_2 U \tag{10}$$

where, m_1 and m_2 are the coefficients for characterizing the mesh. To account for the resistance variation due to the mesh size, Eq. (10) can be expanded as

$$R_{mesh} = m_1 \eta^{-m1p} + m_2 \eta^{-m2p} U \tag{11}$$

where η^{-m1p} and η^{-m2p} (see nomenclature table) reflects the inverse proportionality between flow resistance and pore size. From Eq. (9) and Eq. (11), the mesh resistance parameter A can be estimated:

$$A = (m_1 \eta^{-m1p} + m_2 \eta^{-m2p} U)/e \tag{12}$$

For the column test, U in Eq. (4) is the rate of change of column height $-dh/dt$. Substituting Eq. (12) into Eq. (4) and rearranging gives the governing equation for height (water level) variation in a clean water drainage test with negligible wall effects:

$$\frac{dh}{dt} = -\frac{\rho g \Delta h}{\mu(m_1 \eta^{-m1p} + m_2 \eta^{-m2p} U)} \tag{13}$$

The solution of Eq. (13) provides the rate of change of height, which was utilized to evaluate the mesh resistance coefficients ($m_1, m1p, m_2, m2p$) by simultaneously fitting the solution of Eq. (13) with seventy drainage test curves (CWDC), as shown in Fig. 5 and Fig. SI1. This approach allows us to properly evaluate mesh resistance as a function of flow velocity and mesh size.

3.2. Evaluation of cake filtration coefficients for RBF sizing (BCE method)

Once clean mesh water parameters are estimated and fixed, Eq. (14) can be used to estimate the remaining model parameter with wastewater experiments using a column test apparatus. This approach focuses on evaluating the cake resistance coefficients using the drainage column test. We assess these coefficients by fitting the drainage column test data with the solution of the following expression:

$$\frac{dh}{dt} = -\frac{\rho g \Delta h}{\mu A e^{e^{CFV.B}}} \tag{14}$$

where, B is expanded using Eq. (5).

To evaluate the cake resistance coefficients, all the 29 column tests (WWDC-1) results were used to obtain a single set of coefficients for Eq. (14). Fig. 6 shows the wastewater column tests for 9 different combinations of mesh size and TSS_{in} along with the fitted model results. The sound agreement between the experimental data and model predictions shows that this approach is suitable to account for mesh size and TSS_{in} variations using a single set of coefficients, thus making the model more generic and widely applicable. Furthermore, Fig. 6 also includes the corresponding clean water column tests with model predictions, which further depicts the generic nature of the developed filtration model.

Using the wastewater sieve test results, we can fit Eq. (7) to obtain the TSS_{out} coefficients. To demonstrate the efficacy of this approach, we used a batch of sieve tests (WWS) involving variations in mesh size, TSS_{in}, and CFV. To evaluate a single set of TSS_{out} coefficients, the sieve test results were fitted together, as shown in Fig. 7. Using this set of coefficients, we can now predict TSS_{out} for different mesh sizes and TSS_{in}. Moreover, the incorporation of CFV allows us to confidently

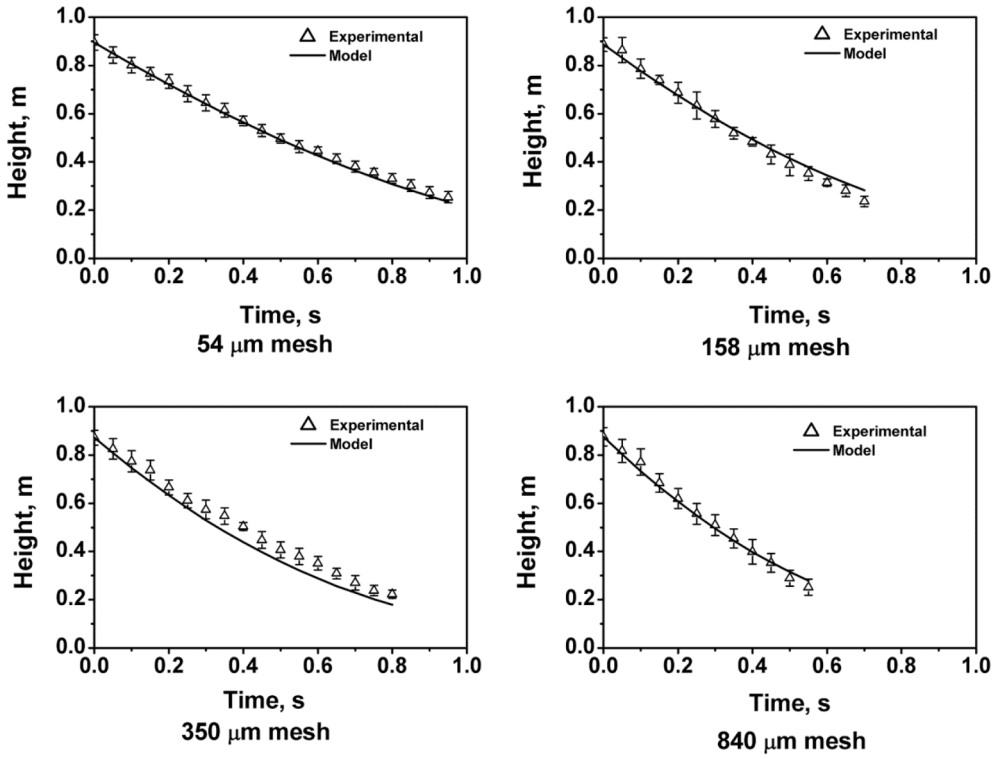

Fig. 5. Clean water gravity drainage column tests for various mesh sizes and model predictions (Eq. (13)).

predict the TSS_{out} , based on various levels of filtered flows.

3.3. Evaluation of cake filtration coefficients (PCE method)

Further calibration of the cake filtration coefficients can be obtained using pilot data. To evaluate the cake resistance coefficients using this approach, logged data of belt speed, water level, TSS_{in}, and flow rate (Q_{exp}) were collected and used for calibration. Belt speed, TSS_{in}, and water level data were used as inputs to solve Eq. (4) to obtain the Q_{model}. The values of resistance coefficients were iteratively refined using an optimization algorithm until the error between Q_{model} and Q_{exp} is minimized. Fig. 8 shows the potential of this approach by plotting the calibrated model results against the pilot data obtained with and without pre-treatment by polymer, which was obtained from the RBF pilot unit operated at Pottersburg WWTP (PC). It also shows that the modeling framework developed in this study that takes simultaneously into account suspended solids concentration, particle size, mesh sizes and polymer doses work remarkably well for the tested range of conditions.

Logged pilot data were also used to predict effluent suspended solids concentration (TSS_{out}). To evaluate TSS_{out} equation coefficients, Q_{exp},TSS_{in} and TSS_{out} were used in a similar manner as described before for the case of estimation of cake resistance coefficients. Fig. 9 shows the calibrated TSS_{out} equation results against the experimental data, confirming that the calibrated TSS_{out} equation allows for accurate predictions of solids separation efficiency for varying polymer doses and flow rates.

With all the required coefficients finally estimated and known, the filtration model can now be used for simulating different operating conditions as a function of process and system variables. In this respect, we simulated the effect of varying belt speeds, polymer concentrations, TSS_{in}, and mesh sizes. Fig. 10 reports the effect of mesh size and TSS_{in} on flow rate and removal efficiency. With increasing mesh size, the flow rate increases, while removal efficiency decreases. Moreover, an increase in TSS_{in} improves removal efficiency at the expense of a reduction in flow rate. The model was also able to predict the effect of pre-treatment with different polymer concentrations, as shown in Fig. SI2 (see supporting information file). With the increase in belt speed, the flow rate tends to increase while removal efficiency tends to decrease. As expected, an increase in polymer concentration results in higher removal efficiency at the expense of a drop in system capacity and flow rate. Thus, the model enables accurate sizing as predictions can be made with a satisfactory degree of accuracy for different processes and design conditions.

3.4. Model-based RBF sizing: The BCE method and the PCE method

3.4.1. The BCE method

To validate this approach, the resistance coefficients were obtained by fitting 11 drainage column tests together (WWDC-2), as shown in Fig. 11, while the sieve tests (WWS) shown in Fig. 7 were used for the evaluation of TSS_{out} coefficients. We observed deviations between the model predictions and pilot data (PV), as shown in Fig. 12. This deviation occurs due to the differences in water quality between the bench-scale data (column and sieve tests) and the pilot data, as they were carried out at different times. Although PV, WWDC-2, and WWS datasets were produced at the Pottersburg facility, but not at the same time, which means that the wastewater quality may not be identical for the three datasets. Ideally, all the tests and data collection activities should be done simultaneously to avoid the differences in wastewater quality. However, even in such a case, it would be challenging to have perfectly matching results because column and sieve tests cannot accurately capture the real-time fluctuations in wastewater quality. Despite such limitations, the BCE method produces the root mean square error of flow and TSS_{out} equal to 6.58 L/s and 23.16 mg/L, respectively.

3.4.2. The PCE method

To validate the PCE approach, we used the PC dataset (Figs. 8 and 9). The model predictions are shown in Fig. 13, which shows good agreement with the PV dataset. Interestingly, both calibration and validation datasets were generated at Pottersburg WWTP at different times, yet the calibration data captured the variations in wastewater qualities resulting in accurate predictions. This results in the root mean square error of

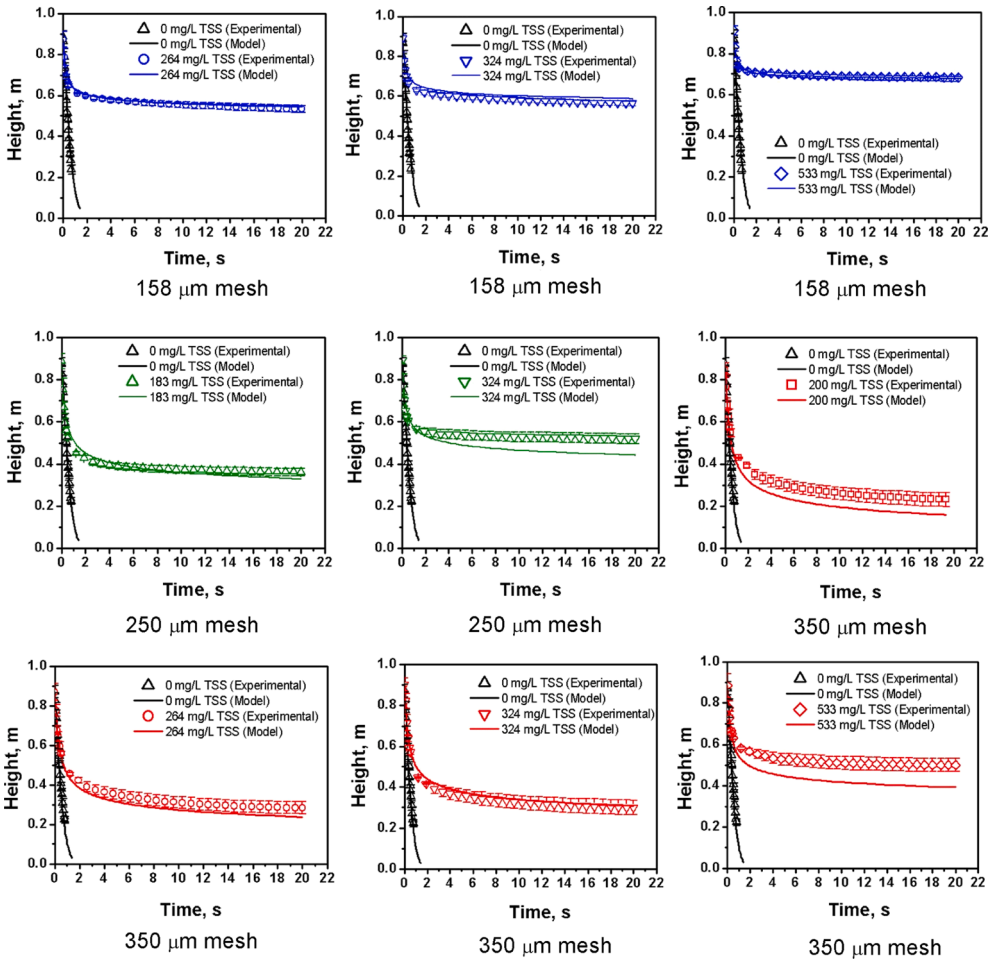

Fig. 6. Wastewater gravity drainage column tests for various mesh sizes and TSS_{in}. The color markers represent wastewater column tests, and the black markers represent the clean water column tests.

flow and TSS_{out} equal to 2.02 L/s and 9.19 mg/L, respectively, which is significantly less compared to the BCE method.

3.4.3. *Application of the PCE method to other international locations*

One key aspect of the developed model is its capability to simulate RBF systems across different geographic locations. Thus, it is essential to validate the model for different WWTPs around the world. Fig. 14 shows the model results obtained after calibrating it with the corresponding pilot data for global locations such as Korea, USA, and Australia. The results show that the RBF model can capture the filtration process for all the locations accurately by only using the relevant pilot data. It should be noted that these datasets were collected before the present model was developed and used different mesh sizes and differing qualities of wastewater. Fig. 14 also shows the general applicability of the model, where it can be used to simulate the filtration process of diverse qualities of wastewater around the world. The plot also shows that using the pilot data, the filtration model can capture the quality of wastewater without any sieve and column drainage tests, which shows the generic nature of the model.

3.5. *Guidance for future pilot studies via model based analysis*

The success in calibrating the model against pilot data shown in the previous sections raises a question: how much data is required to satisfactory retrieve the model coefficients and to enable accurate sizing? To answer this question, we carried out model simulations in two ways. In the first case (scenario 1), we generated numerical experiments by running the RBF model based on naturally occurring variations in flow rate and TSS_{in} obtained from the influent data file of the Benchmarking Simulation Model #2 (BSM2) by Jeppsson et al. [23]. This case simulates RBF pilot testing where the inflow to the pilot is dictated by gravity. In the second case (scenario 2), we generated numerical experiments by assuming certain flowrate patterns. This case simulates RBF pilot testing where the inflow to the pilot is dictated by a pump while the TSS_{in} is still obtained from the BSM2 influent data. These two ways of operations reflect how the RBF units can be piloted in real site (using gravity in the first case, and pumped flow in the second case). In both scenarios, the upstream water level is kept to a desired setpoint by adjusting belt speed, to simulate the control logic implemented in the Salsnes RBF units. The following simulation procedure was carried out:

1) Running the filtration model to estimate ω and TSS_{out}. The model was simulated using the coefficients that were obtained by calibrating a usual pilot RBF data;
2) Added random noise to each of the RBF system parameters such as Q_{model}, TSS_{in}, TSS_{out}, ω and upstream water level to transform clean data into realistic RBF data using as uncertainty the standard deviation from real pilot RBF data;
3) Used the system data generated in step 2 to re-evaluate the model coefficients by error minimization using an optimization method automatically implemented in the code;
4) Compared estimated with a-priori known pilot coefficients to determine estimation errors.

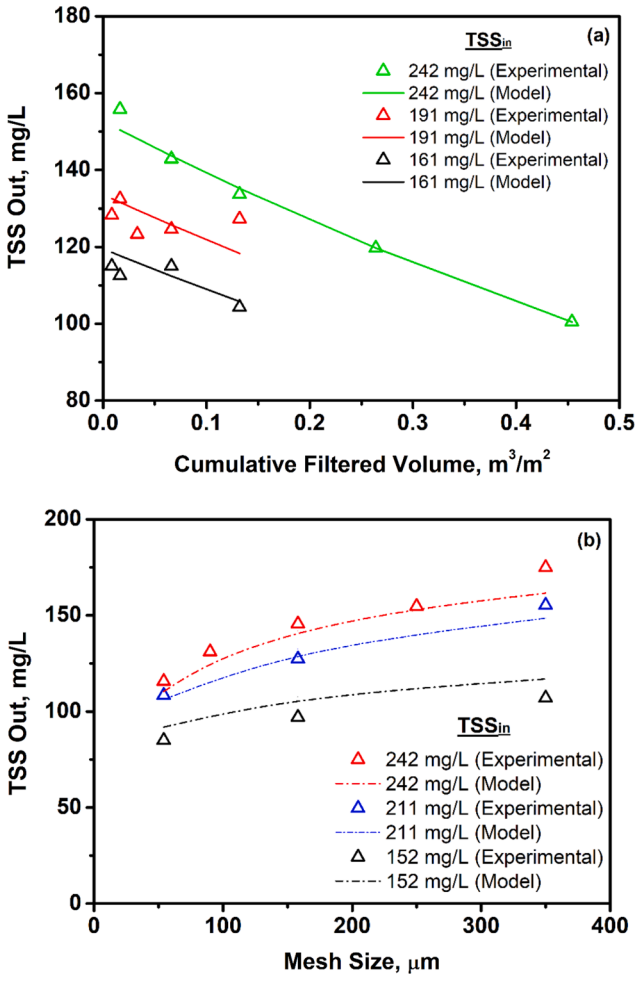

Fig. 7. Sieve test results for TSS_{out} as a function of TSS_{in} and a) *CFV* b) mesh size.

In scenario 1, 8 different sampling events were simulated. The first sampling event duration was of 1 h, having 4 sampling points with 15-minute intervals. The second sampling event duration was of 2 h. By doubling the sampling event duration in this manner, the 8th sampling event lasted for 128 h, having 512 sampling points. In scenario 2, the flow rate was gradually increased. Consequently, each row in Table 1 represents an individual sampling event with a given amount of data.

All events in scenarios 1 and 2 were simulated using 0%, 10%, and 20% levels of random noise, which covers the uncertainty levels commonly observed in pilot studies. Adding no noise to the model parameters (0% random disturbance) allowed us to retrieve the base parameters with fewer sampling points at almost 100% accuracy, which verified the suitability of the calculation approach.

Based on our model-based analysis, testing the system with scenario 1 (gravity fed RBF unit) allowed rapid convergence towards the a-priori assigned parameters. Indeed, with a 20% noise level (Table SI3), 8 h of sampling (or 32 sample points) were already sufficient to retrieve the model parameters with a satisfactory level of accuracy (Table SI3). In the case of scenario 2 (pump-fed RBF unit), at least 3 flowrate and 3 h of sampling at each flowrate are required to achieve a similar level of accuracy of scenario 1 (Table SI4). Increasing the number of flowrates and the hours of sampling did not seem to considerably improve the estimate of the model parameters.

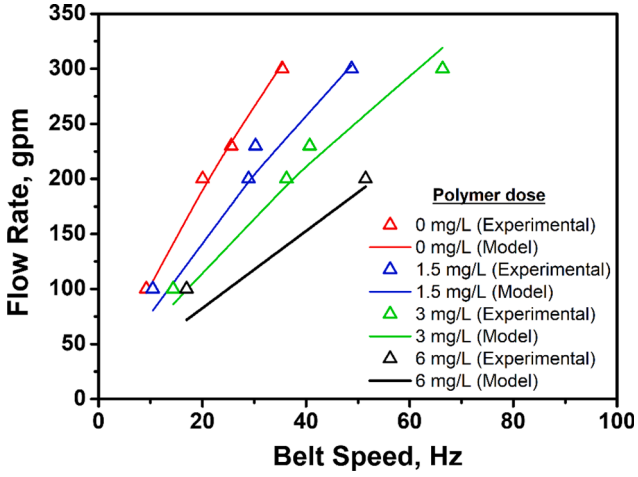

Fig. 8. Average flow rate as a function of belt speed for various polymer doses.

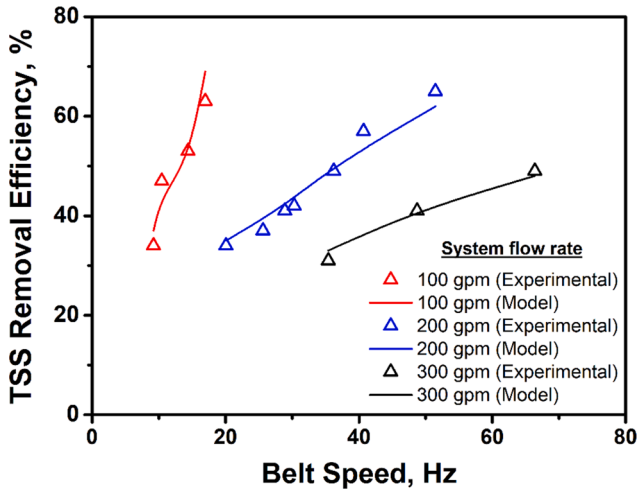

Fig. 9. Average *TSS* removal efficiency as a function of belt speed for various flow rates.

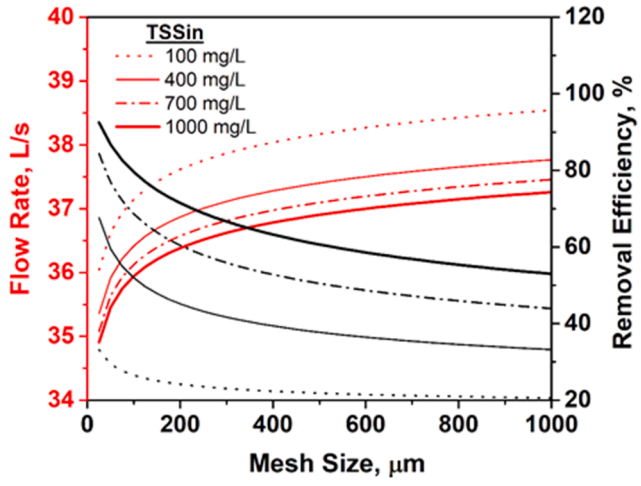

Fig. 10. Predicted flow rates and *TSS* removal efficiency as a function of mesh size and TSS_{in}.

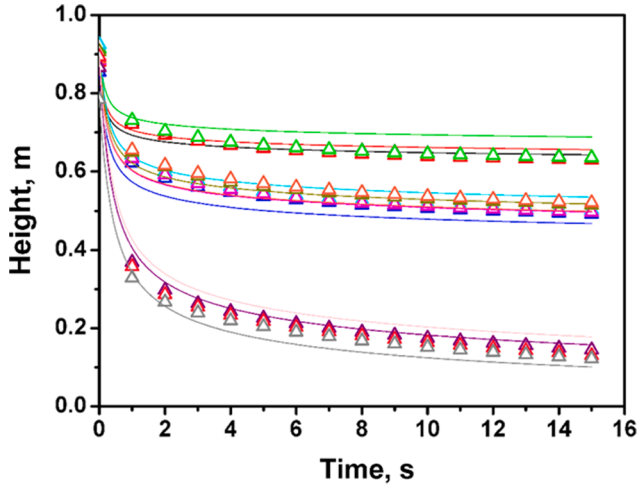

Fig. 11. Drainage column tests with fitted model results. The same color markers represent column test data, and the corresponding color line shows the predicted model results. The entire set of 11 drainage tests having different TSS_{in} was fitted together to obtain the model predictions.

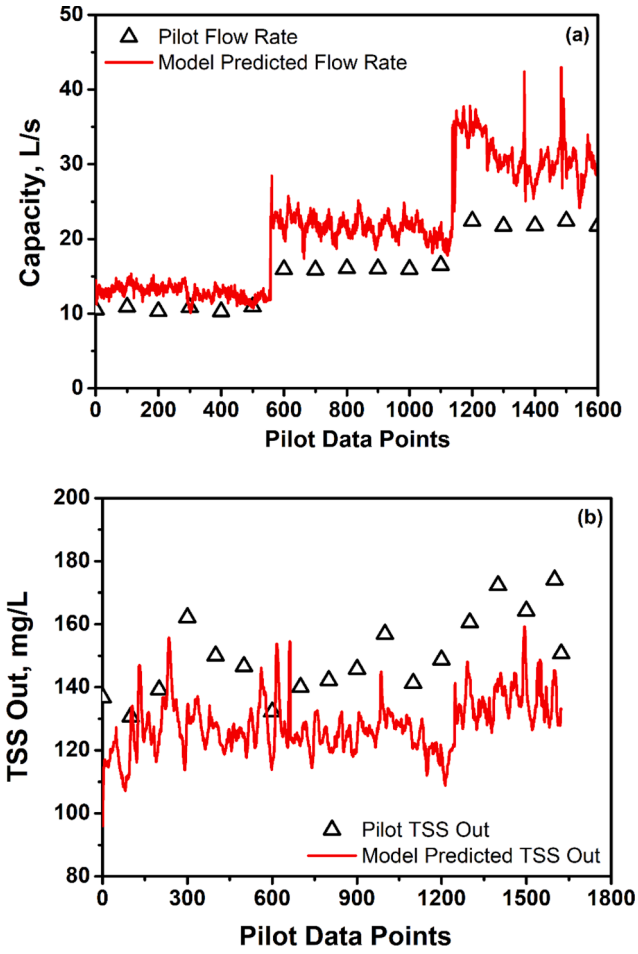

Fig. 12. Model prediction of a) flow rate b) TSS_{out} against the Pottersburg WWTP data. The model was fitted with column drainage and sieve tests.

4. Conclusions

Overall, the filtration model developed in this study was found to be suitable and highly adaptable to a variety of real operating and testing conditions, as shown by the extensive validation studies carried out in this paper. Specifically, results reported in this manuscript allow to draw the following conclusions:

- Wastewater drainage column and sieve tests can be used as a first approximation to obtain the water-quality-specific model coefficient required for RBF sizing, with relative error (at average flow and influent total suspended solids concentration) of 33% and 14% for filter capacity and effluent total suspended solids, respectively.
- Accessing pilot data enhance model calibration allows further reducing the RBF sizing uncertainty considerably, with the relative error not exceeding 9% for filter capacity and 5% for effluent total suspended solids. Furthermore, the model developed in this study was able to perform well also against pilot data obtained from three international locations (Korea, USA, and Australia).
- The validated model provided useful guidance for future pilot studies. Specifically, it is recommended that, in the case of gravity-fed RBF unit, at least 8 h of piloting time (with data acquisition frequency of 15 min) are employed to allow a satisfactory estimate (with a 20% uncertainty) of the filtration parameters. If the same level of uncertainty is targeted with pump-fed RBF unit, the RBF system must be tested with at least three distinct flowrate and for more at least three hours per flow.

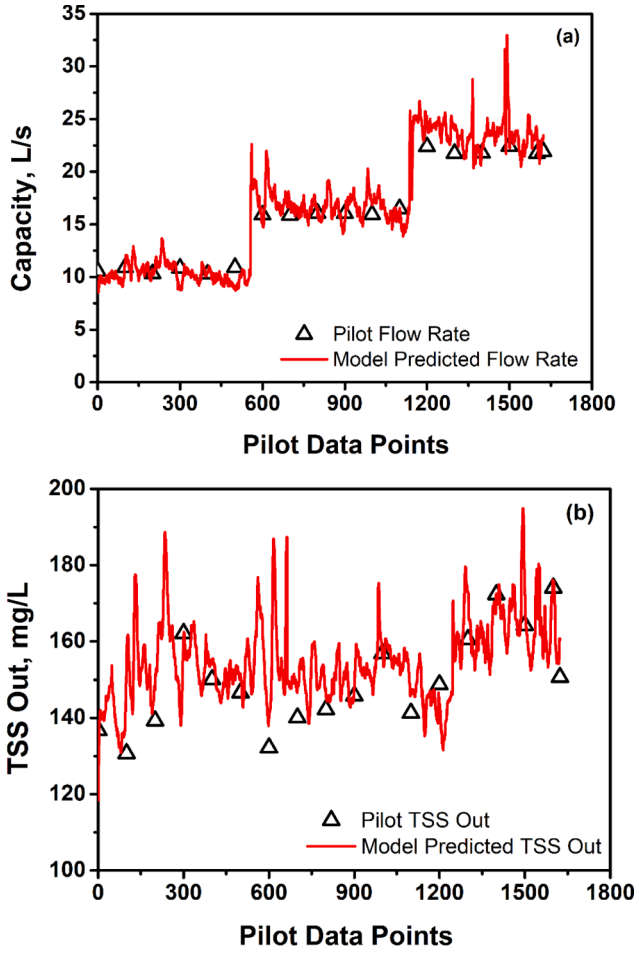

Fig. 13. Model prediction of a) flow rate b) TSS_{out} against the Pottersburg validation data.

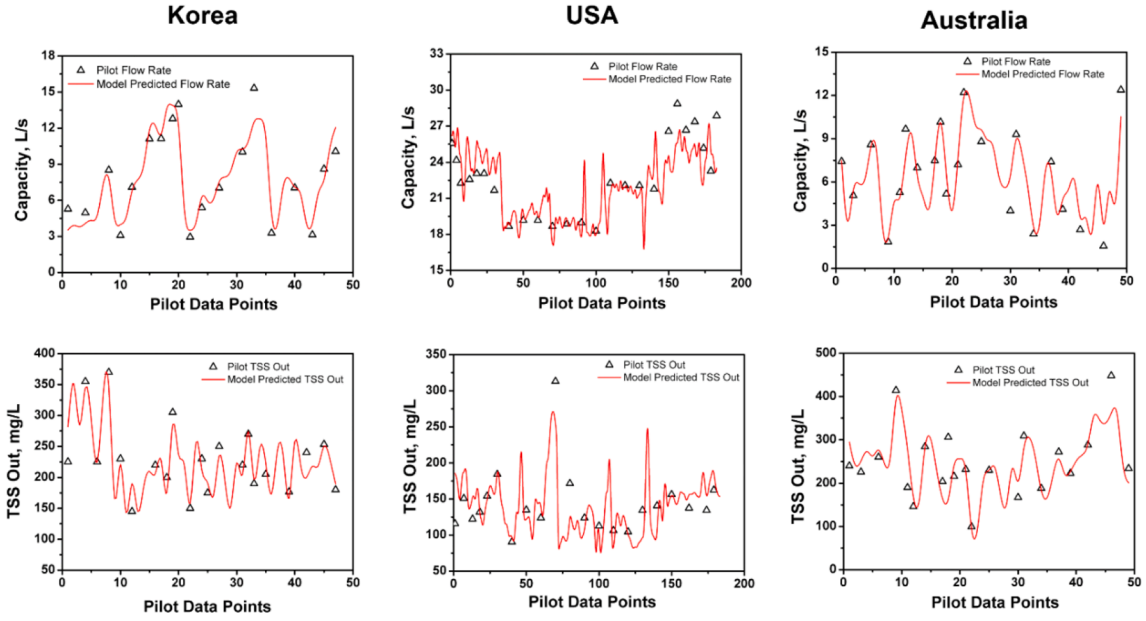

Fig. 14. Model predictions against pilot data at different locations.

Table 1
Sampling points for scenario 2 with a controlled flow rate. In each pattern, flow rate is increased in steps. Pattern-1: constant flow rate of 60 L/s, Pattern-2: [30, 90] L/s, Pattern-3: [30, 60, 90] L/s, Pattern-4: [30, 50, 70, 90] L/s, Pattern-5: [30, 45, 60, 75, 90] L/s.

Sampling duration (h)	Total sampling points				
	Pattern-1	Pattern-2	Pattern-3	Pattern-4	Pattern-5
1	4	8	12	16	20
2	8	16	24	32	40
3	12	24	36	48	60
4	16	32	48	64	80
5	20	40	60	80	100

CRediT authorship contribution statement

Furqan Ahmad Khan: Investigation, Methodology, Visualization, Writing - original draft. **Pankaj Chowdhury:** Investigation, Methodology, Validation, Visualization, Writing - review & editing. **Francesca Giaccherini:** Validation, Writing - review & editing. **Anthony Gerald Straatman:** Methodology, Project administration, Supervision, Writing - review & editing. **Domenico Santoro:** Conceptualization, Methodology, Supervision, Writing - review & editing.

Declaration of Competing Interest

The authors declare that they have no known competing financial interests or personal relationships that could have appeared to influence the work reported in this paper.

Acknowledgements

The authors gratefully acknowledge the support from the Lambton Water Center in Sarnia, Ontario, Canada in collecting column and sieve tests data. Dr. Siva Sarathy is also kindly acknowledged for his feedback and for offering critical review to the experimental methods.

Appendix A. Supplementary material

Supplementary data to this article can be found online at https://doi.org/10.1016/j.seppur.2021.118777.

References

[1] A.S. Ahmed, G. Bahreini, D. Ho, G. Sridhar, M. Gupta, C. Wessels, P. Marcelis, E. Elbeshbishy, D. Rosso, D. Santoro, Fate of cellulose in primary and secondary treatment at municipal water resource recovery facilities, Water Environ. Res. 91 (2019) 1479–1489.
[2] C.R. Behera, D. Santoro, K.V. Gernaey, G. Sin, Organic carbon recovery modeling for a rotating belt filter and its impact assessment on a plant-wide scale, Chem. Eng. J. 334 (2018) 1965–1976.
[3] C.J. Ruiken, G. Breuer, E. Klaversma, T. Santiago, M.C.M. Van Loosdrecht, Sieving wastewater–Cellulose recovery, economic and energy evaluation, Water Res. 47 (2013) 43–48.
[4] D. Ho, Z. Scott, S. Sarathy, D. Santoro, Innovative Wastewater Treatment & Resource recovery Technologies: Impacts on Energy, Economy and Environment, IWA Publishing, London, UK, 2017.
[5] C. Tien, B.V. Ramarao, Revisiting the laws of filtration: An assessment of their use in identifying particle retention mechanisms in filtration, J. Membr. Sci. 383 (2011) 17–25.
[6] E.I. Vorobjov, J.V. Anikeev, V.M. Samolyotov, Dynamincs of filtration and expression: new methods for combined analysis and calculation of the processes with due account of the cake consolidation dynamics and the filter medium compressibility, Chem. Eng. Process. 32 (1993) 45–51.
[7] N.M. Abboud, M.Y. Corapcioglu, Modeling of compressible cake filtration, J. Colloid Interface Sci. 160 (1993) 304–316.
[8] S.A. Wells, Analytical modeling of cake filtration, Adv. Filtration Separat. Technol. 13a (1999) 158–165.
[9] S.A. Wells, Variation of Constitutive Model Formulation on Analytical Cake Filtration Models, Advances in Filtration and Separation Technology, American Filtrations and Separations Society, 2000.
[10] R. Bai, C. Tien, Further work on cake filtration analysis, Chem. Eng. Sci. 60 (2005) 301–313.
[11] C. Tien, Cake filtration research—a personal view, Powder Technol. 127 (2002) 1–8.
[12] S.-K. Teoh, R.B.H. Tan, C. Tien, Analysis of cake filtration data—a critical assessment of conventional filtration theory, AIChE J. 52 (2006) 3427–3442.
[13] C. Tien, B.V. Ramarao, On the analysis of dead-end filtration of microbial suspensions, J. Membr. Sci. 319 (2008) 10–13.
[14] C. Tien, R. Bai, An assessment of the conventional cake filtration theory, Chem. Eng. Sci. 58 (2003) 1323–1336.
[15] C. Tien, B.V. Ramarao, R. Yasarla, A blocking model of membrane filtration, Chem. Eng. Sci. 111 (2014) 421–431.
[16] S. Osterroth, C. Preston, B. Markicevic, O. Iliev, M. Hurwitz, The permeability prediction of beds of poly-disperse spheres with applicability to the cake filtration, Sep. Purif. Technol. 165 (2016) 114–122.
[17] C.-C. Ho, A.L. Zydney, A combined pore blockage and cake filtration model for protein fouling during microfiltration, J. Colloid Interface Sci. 232 (2000) 389–399.
[18] C.T. DeGroot, E. Sheikholeslamzadeh, D. Santoro, S. Sarathy, T.-O. Lyng, Y. Wen, F. Daynouri-Pancio, D. Rosso, Dynamic modeling of rotating belt filters enables design exploration and advanced sizing with varying influent conditions, Proc. Water Environ. Federation 2016 (2016) 1158–1168.
[19] A. Sherratt, C.T. DeGroot, A.G. Straatman, D. Santoro, Numerical modeling and control of solids separation using continuously moving fine mesh filters, Chem. Eng. Sci. 195 (2019) 881–893.
[20] R. Boiocchi, C.R. Behera, A. Sherratt, C.T. DeGroot, K.V. Gernaey, G. Sin, D. Santoro, Dynamic model validation and advanced polymer control for rotating belt filtration as primary treatment of domestic wastewaters, Chem. Eng. Sci. 217 (2020) 115510.
[21] Salsnes Filter, 2020. Retrieved from https://www.salsnes-filter.com/products/ (accessed 15 Nov 2020).
[22] A. Sherratt, C.T. DeGroot, A.G. Straatman, D. Santoro, A numerical approach for determining the resistance of fine mesh filters, Trans. Can. Soc. Mech. Eng. 43 (2018) 221–229.
[23] U. Jeppsson, M.N. Pons, I. Nopens, J. Alex, J.B. Copp, K.V. Gernaey, C. Rosen, J. P. Steyer, P.A. Vanrolleghem, Benchmark simulation model no 2: general protocol and exploratory case studies, Water Sci. Technol. 56 (2007) 67–78.